PERGAMON

Acta mater. Vol. 47, No. 9, pp. 2777–2785, 1999
© 1999 Acta Metallurgica Inc.
Published by Elsevier Science Ltd. All rights reserved
Printed in Great Britain
1359-6454/99 $20.00 + 0.00

PII: S1359-6454(99)00122-6

DEBONDING BEHAVIOR BETWEEN β-Si_3N_4 WHISKERS AND OXYNITRIDE GLASSES WITH OR WITHOUT AN EPITAXIAL β-SiAlON INTERFACIAL LAYER

E. Y. SUN†[1]‡, P. F. BECHER[1], C.-H. HSUEH[1], G. S. PAINTER[1], S. B. WATERS[1], S.-L. HWANG§[1] and M. J. HOFFMANN[2]

[1]Metals and Ceramics Division, Oak Ridge National Laboratory, Oak Ridge, TN 37831-6068, U.S.A. and [2]University of Karlsruhe, Institute of Ceramics in Mechanical Engineering, Karlsruhe, Germany

(Received 13 January 1999; accepted 1 April 1999)

Abstract—In order to gain insight on the influence of intergranular glass on the fracture toughness of silicon nitride, the debonding behavior of the interface between the prismatic faces of β-Si_3N_4 whiskers and oxynitride glasses was investigated in model systems based on various Si–(Al)–Y(Ln)–O–N (Ln: rare-earth) oxynitride glasses. It was found that while the interfacial debonding strength increased when an epitaxial β'-SiAlON layer grew on the β-Si_3N_4 whiskers, the critical angle for debonding was lowered with increasing Al and O concentrations in the SiAlON layer. Only in the absence of a SiAlON epitaxial layer, were debonding conditions altered by residual stresses imposed on the interface due to thermal–mechanical mismatch. A possible explanation for the effect of SiAlON formation and its composition on the debonding behavior is suggested by first-principles atomic cluster calculations. It is concluded that by tailoring the densification additives and hence the chemistry of the intergranular glass, it is possible to improve the fracture resistance of silicon nitride. © *1999 Acta Metallurgica Inc. Published by Elsevier Science Ltd. All rights reserved.*

Key words: Structural ceramics; Interface; Fracture toughness; Indentation

1. INTRODUCTION

It is now well known that the toughness of silicon nitride can be improved by inducing a self-reinforced microstructure, ideally with elongated β-Si_3N_4 grains embedded in a fine-grained matrix [1–5]. These elongated β-Si_3N_4 grains can act as reinforcements, provided that the interface between the elongated grains and the surrounding matrix is controlled so that toughening mechanisms such as crack deflection and crack bridging can be activated upon failure [4, 6]. The key issue here is the strength of the interface between the elongated β-Si_3N_4 grains and the surrounding intergranular glassy phase. To promote the crack deflection and the crack bridging processes, it is necessary for the interface between the β-Si_3N_4 and the intergranular glass to debond as the crack front approaches. Only when the interface debonds, will the reinforcements deflect the crack tip and bridge the crack opening behind the crack front. Therefore, the debonding behavior of the interface between the β-Si_3N_4 and the intergranular glass phase is of great importance, not only for improving the mechanical performance of silicon nitride but also for obtaining a fundamental understanding of the crystalline/glass interface that is ubiquitous in ceramic systems.

In materials with a reinforced microstructure, the interfacial debonding behavior can be influenced by both the interfacial microstructure/chemistry and the thermal expansion mismatch stresses imposed on the interface [7]. Earlier studies have shown that densification additives used in processing silicon nitrides can affect the material's failure mode [8–10]. Different toughness values and interfacial failure behaviors have been observed in silicon nitrides with similar self-reinforced microstructures when different alumina-to-yttria ratios were employed [11]. However, due to the complexity of the material system, it is difficult to establish a one-to-one correlation between the sintering additives and the interfacial debonding behavior. To overcome this problem, a model system has been employed by dispersing β-Si_3N_4 whiskers in oxynitride glasses [12, 13]. With this technique, the influence of densification additives on the debonding behavior at interfaces between the β-Si_3N_4 whiskers and the oxynitride glasses can be investigated by systematically varying the glass composition. Earlier results on the debonding behavior in Si–Al–Y oxynitride glasses have been reported in previous publications [12, 13]. This paper reports new find-

†To whom all correspondence should be addressed.
‡Present address: United Technologies Research Center, 411 Silver Lane, MS 129-26, East Hartford, CT 06108, U.S.A.
§Present address: Kaohsiung Polytechnic Institute, Kaohsiung, Taiwan.

Table 1. The whisker content, the glass composition, the processing parameters, and the measured θ_{crit} values of the β-$Si_3N_{4(whisker)}$/oxynitride-glass samples

Sample		Whisker (vol.%)	Composition (eq.%)					Temp. (°C)	Time at temp. (min)	θ_{crit} (deg)
			Si	Al	Y or Ln	O	N			
Group I	AlY05	5	55	25	20	95	5	1525	6	75
	AlY10	5	55	25	20	90	10	1700	1	70
	AlY20-I	5	55	25	20	80	20	1700	6	55
	YAl10	5	55	10	35	90	10	1650	1	70
	YAl20-I	5	55	10	35	80	20	1700	8	72
	AlY20-II	5	55	25	20	80	20	1600	60	52
	YAl20-II	5	55	10	35	80	20	1600	60	50
Group II	La	5	57	0	43	79	21	1700	4	65
	LaAl	2.64	46	27	27	70	30	1680	30	50
	YbAl	3.29	42	29	29	76	24	1680	30	57

ings in the Si–Al–Y system and also the debonding behavior in rare-earth based oxynitride glass systems. In addition, relationships between the debonding behavior in the whisker/glass model systems and that in self-reinforced silicon nitride ceramics are addressed, the role of residual stresses on the interfacial debonding behavior is discussed and a possible explanation for the effect of the β'-SiAlON composition on the debonding behavior is given.

2. EXPERIMENTAL PROCEDURE

Two groups of oxynitride glasses with dispersed β-Si_3N_4 whiskers (ESP grade, UBE) were prepared. The whisker content, the glass composition and the processing parameters are listed in Table 1. Group I was composed of Y-bearing Si–Al–Y–O–N glasses. Details of the processing procedures can be found in Ref. [12]. Note that samples AlY20-II and YAl20-II were obtained by annealing AlY20-I and YAl20-I under the conditions listed in Table 1. Group II was composed of Ln-bearing Si–(Al)–Ln–O–N glasses. Specimen La was prepared following similar procedures as those for Group I while specimens LaAl and YbAl were prepared following the general procedures described in Ref. [13]. X-ray diffraction analysis was performed on all of the samples to confirm glass formation, complete dissolution of the starting powders and retention of the β-Si_3N_4 whiskers. Compositional uniformity of the glasses, with respect to cation concentrations, was examined using energy dispersive spectroscopy (EDS, Model 400B-1SPT, Noran Instruments, Inc., Middleton, WI) equipped on a scanning electron microscope (SEM, S4100, Hitachi) and electron probe microanalyses (EPMA) (Superprobe 733, JEOL, Tokyo, Japan). The nitrogen and oxygen concentrations in the glasses in selected samples (AlY10, YAl10, La, LaAl, and YbAl) were verified using thermal conductivity and infrared detection methods.† Quantitative compositional analyses of the SiAlON epitaxial layer grown on the β-Si_3N_4 whiskers were conducted using EDS in SEM. EDS spectra were analyzed using the Desk Top Spectrum Analyzer and X-Ray Data Base (DTSA) (National Institute of Standards and Technology, Gaithersburg, MD).

The interfacial debonding behavior in these materials was examined using an indentation–crack-interaction technique. As illustrated by the schematic diagram in Fig. 1(a), an indentation is placed in the glass to induce cracks near a selected whisker. Propagating in the glass and intersecting the longitudinal edge of the whisker, the crack will either deflect at the whisker/glass interface or penetrate the whisker, depending on the angle of incidence (θ) [14]. For a specific interface, it becomes increasingly more difficult for a crack to deflect and travel along the interface as θ is increased towards 90° [14]. By measuring the interface debond length, l_{db}, and plotting the data vs θ, the maximum angle of incidence for the onset of interfacial debonding (θ_{crit}) can be determined, as shown in Fig. 1(b). The interfacial debonding energy in different systems can be assessed by comparing the θ_{crit} and l_{db} values. In general, the interfacial debonding energy decreases as θ_{crit} increases. For a selected θ value, an increase in l_{db} also reflects a decrease in the debonding energy. Between these two parameters, θ_{crit} is the prime factor as it dictates the fraction of whiskers (or elongated grains) present that have the potential to deflect the crack and thus serve as crack bridging reinforcements. Given randomly oriented whiskers (or elongated grains), if θ_{crit} is very large, then most of the whiskers (or elongated grains) could participate in the toughening process. If θ_{crit} is small, only a small percentage of the whiskers (or elongated grains) will be favorably oriented. The debond length, l_{db}, is a less significant but still important factor, as larger l_{db} values for a given θ value will produce greater frictional bridging and, potentially, larger pull-out contributions [15].

The indentation system used for this debonding study consists of three major components: the indenter, an optical microscope (Optiphot 100S, Nikon, Japan) equipped with a CCD camera for

†Analyses conducted by LECO Analytical Lab, St. Joseph, Michigan, U.S.A.

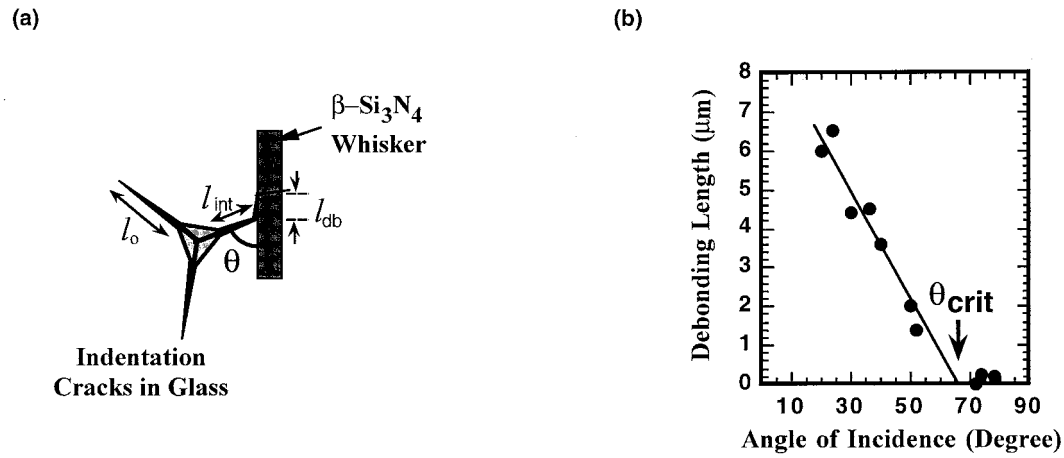

Fig. 1. (a) Schematic diagram of the debonding experiment, showing how the interfacial debonding behavior was examined using an indentation–crack-interaction technique. (b) Data analyses of the debonding experiment. Critical angle θ_{crit} was determined by plotting l_{db} vs θ.

remote viewing, and a precision table that transports the specimen between the microscope and the indenter. The entire system is suspended on a vibration isolation table. The specimen was mounted on the x–y precision table so that its position relative to the microscope and the indenter can be adjusted. During the experiment, the indentation site was first selected under the optical microscope. The indentation site should be close to a β-Si_3N_4 whisker so that one indentation crack would propagate towards the whisker/glass interface of interest. Once positioned, the specimen was transported to the indenter and an indentation was made using a cube-corner diamond indenter. A fixed load, ranging from 25 to 35 g depending on the hardness of each individual oxynitride glass system, was applied for each glass system using a piezoelectric transducer. Typically about 100 indentations were induced in each specimen. Usually only half of the indentation cracks actually interacted with the whisker/glass interfaces due to the small size of the β-Si_3N_4 whisker, the limited indentation crack length, the imperfect alignment and thermal drifting. The specimen was then carbon coated and examined using high-resolution SEM. The debond length (l_{db}) and the angle of incidence (θ) were measured from the SEM images. Precaution was paid to ensure that no other whiskers intersected the interface of interest and the size of the whisker and the distance from the indentation to the interface were consistent from one measurement to another. Data were only collected from interfaces that intersected the crack with $l_{int}/l_0 \sim 0.5$ (l_{int}: the distance between the corner of the indentation impression and the intersection, and l_0: the distance between the corner of the indentation impression and the crack tip when the crack does not intersect with an interface, as shown in Fig. 1). Sites where cracks simply arrested at the interface were excluded from the measurements. Due to these precautions, usually 10–20 data points could be gathered from the ~50 crack/whisker interaction sites. Each data point is an individual measurement in nature. In this sense, it is difficult to provide error bars with the data sets. However, it was noticed during the experiment that in each sample, results were reproducible. In other words, if two indentation cracks approached whiskers at similar angles, the debonding lengths measured were comparable when both interactions satisfied the conditions mentioned above.

3. RESULTS

3.1. Y-Bearing Si–Al–Y–O–N glasses

The interfacial debonding behavior in the β-Si_3N_4/Si–Al–Y–O–N glass systems processed at high temperatures for a short period of time (AlY05, AlY10, AlY20-I, YAl10 and YAl20-I, Table 1) has been reported in detail in a previous publication [12] and is briefly summarized here. It was found that the glass composition had a profound influence on the interfacial debonding behavior. Glasses with higher Y:Al ratios (e.g. YAl systems) and those with lower Y:Al ratios (e.g. AlY systems) and low nitrogen contents ($\leq$10 eq.%) exhibited similar θ_{crit} values (~70°); but the AlY20-I system with both a high Al:Y ratio and a high nitrogen concentration exhibited a significantly lower θ_{crit} value (~50°), Table 1. Electron microscopic studies revealed formation of a β'-SiAlON layer at the Si_3N_4/glass interface in system AlY20-I, which was absent in the other systems [12, 16]. These findings indicated an increase in interfacial debonding strength with the formation of an interfacial SiAlON layer.

Following this early work, SiAlON layer formation and its influence on the interfacial debonding strength were studied further. According to phase diagrams, formation of the β'-SiAlON phase from the Si–Al–Y oxynitride glasses is thermodyna-

Table 2. Measured thermal and mechanical properties of the oxynitride glasses and the β-Si_3N_4 crystal, and the calculated compressive radial residual stresses imposed on the whisker/glass interfaces

Sample	α (10^{-6}/°C)	T_g (°C)	E (GPa)	Compressive radial residual stress (MPa)
AlY05	5.30	895	132	292
AlY10	5.25	915	144	316
AlY20-I	5.17	950	158	346
YAl10	6.66	970	152	513
YAl20-I	6.38	1005	163	529
AlY20-II	5.17	950	158	346
YAl20-II	6.38	1005	163	529
La	7.2	1010	149	589
LaAl	6.5	1030	157	556
YbAl	5.9	990	156	454
β-Si_3N_4	2.01[a]		380	
	2.84[b]		(Ref. [20])	

[a]*a*-Axis.[b]*c*-Axis [19].

mically favorable when the nitrogen content is greater than 16 eq.% [17]. However, under the processing conditions employed (1600–1700°C for several minutes, Table 1), the SiAlON interfacial layer was observed only in system AlY20-I but not in the other high-nitrogen system YAl20-I. The kinetics of the interfacial phase formation via diffusion could have been favored by a lower viscosity in AlY20-I, as indicated by the lower glass transition temperature (T_g) it exhibited as compared to that of glass YAl20-I (Table 2). The increase in T_g value for the YAl20-I glass (≥50°C) is sufficient to lower the glass viscosity substantially and inhibit SiAlON formation for short processing times. However, it is still possible for SiAlON formation to occur in the YAl20 glass with extended holding times at elevated temperatures. Based on this argument, systems AlY20-II and YAl20-II were obtained by annealing AlY20-I and YAl20-I, and the interfacial debonding behavior and microstructures in these two systems were examined. It was found that β'-SiAlON growth on the β-Si_3N_4 whisker indeed occurred in the YAl20 system, as shown in Fig. 2(a). Furthermore, the interfacial debonding behavior of system YAl20 changed dramatically due to the annealing treatment with θ_{crit} decreasing from ~72° before to ~50° after the heat treatment [Fig. 2(b)]. On the other hand, the debonding behavior of system AlY20 remained the same after the annealing treatment. Comparing the data in Table 1, it is noted that the θ_{crit} values are significantly lower in systems with SiAlON formation (AlY20-I, -II and YAl20-II, ~50–55°) than those in the other Si–Al–Y–O–N systems without SiAlON formation (~70–75°). These results confirmed that epitaxial SiAlON growth on the β-Si_3N_4 grains in the Y-bearing Si–Al–Y–O–N glasses strengthens the interfacial bonding between the glass and the β-Si_3N_4 whiskers.

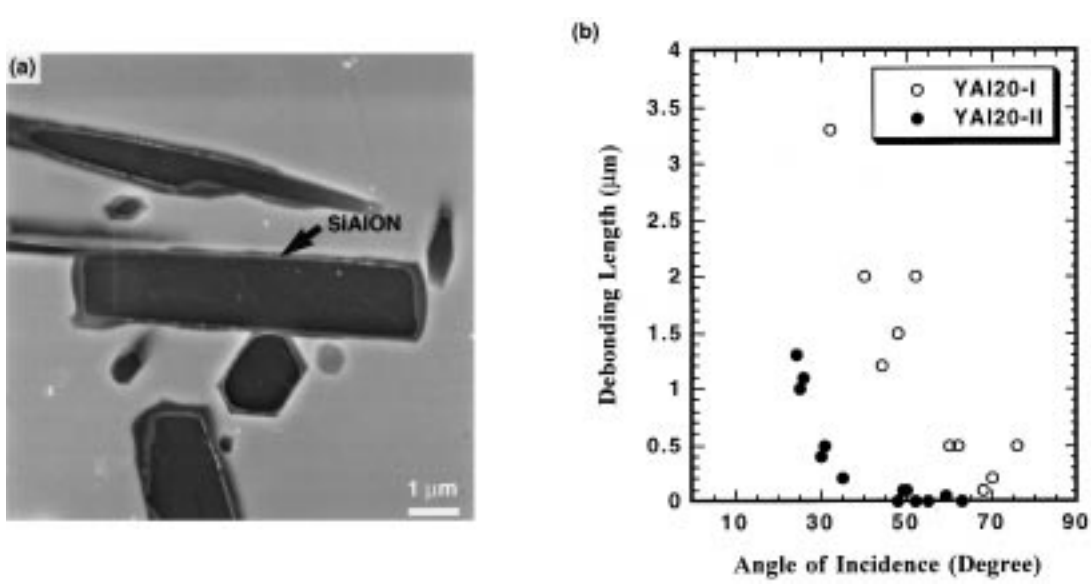

Fig. 2. (a) A β'-SiAlON layer grew on the surface of the β-Si_3N_4 whisker in the YAl20 system due to annealing at 1600°C for 60 min. (b) The interfacial debonding behavior of system YAl20 changed dramatically due to the annealing treatment, with θ_{crit} decreased from ~72° before to ~50° after the heat treatment.

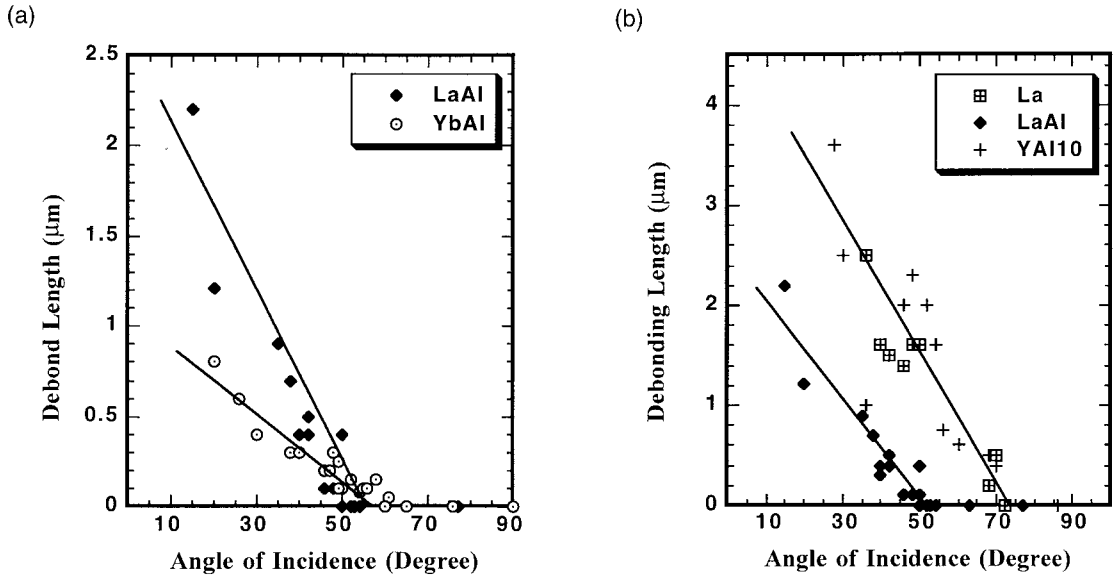

Fig. 3. (a) Interfacial debonding behavior in the Si–Al–La–O–N and Si–Al–Yb–O–N glass systems. The θ_{crit} and l_{db} values are similar to those of the AlY and YAl systems with SiAlON formation. (b) The interfacial debonding was enhanced in the Al-free La systems, as compared to the LaAl system with SiAlON formation. The θ_{crit} and l_{db} values in the Al-free La system were comparable with those in the AlY and YAl systems without SiAlON formation.

3.2. Ln-Bearing Si–Al–Ln–O–N glasses

SiAlON formation had a similar influence on the interfacial debonding energy when rare earth ions were substituted for Y in the Ln-bearing Si–Al–Ln–O–N glass systems. SiAlON epitaxial growth on the Si_3N_4 whiskers occurred in both the LaAl and the YbAl systems. The SiAlON growth band exhibited the same structure as that shown in Fig. 2(a) in the Y-bearing Si–Al–Y–O–N systems. The θ_{crit} and l_{db} values in the LaAl and YbAl systems are similar to those of the AlY and YAl systems with epitaxial SiAlON formation. To exclude the influence of SiAlON layer on the interfacial debonding behavior, an Al-free La system was prepared. The interfacial debonding was enhanced in the Al-free La systems compared to the LaAl system with SiAlON formation [Fig. 3(b)]. Furthermore, the θ_{crit} and l_{db} values in the Al-free La system were comparable with those in the AlY and YAl systems where SiAlON formation is absent, as shown in Fig. 3(b). These results elucidated a fundamental change in the whisker/glass interfacial bonding structure due to the formation of a SiAlON layer on the β-Si_3N_4 whiskers. It is clear that such a microstructural evolution is possible whenever SiAlON formation is thermodynamically favorable.

It is also noted that the interfacial debonding behavior could be modified by employing different rare-earth ions in the Si–Al–Ln–O–N glasses. As shown in Fig. 3(a), the interfacial debond length, l_{db}, for a given θ value increases when the Yb^{3+} ion is replaced by the larger La^{3+} ion, suggesting a weaker interfacial bonding between the β-Si_3N_4 whisker and the Si–Al–La–O–N glass than that between the whisker and the Yb-bearing glasses. Nakayasu *et al.* have performed first-principles molecular orbital calculations on simple cluster models for the interface between the prismatic planes of β-Si_3N_4 and the intergranular glassy films where Ln^{3+} segregated [18]. Their results indicate that the total overlap population of electrons among the clusters decreases as the radius of the Ln^{3+} ion increases, suggesting (1) lower stability of the prismatic plane due to the presence of larger Ln^{3+} ions at the interface and (2) weakened local chemical bonding around larger Ln^{3+} ions at the grain boundaries. Therefore, the strength of bonds across the prism surface to the Si–Al–Ln–O–N glass should decrease with increasing Ln^{3+} ion size, consistent with the present experimental results. However, at this stage, the role of thermal expansion mismatch stresses on the debonding behavior in these two systems is not clear, nor is the extent to which the initial modeling work applies. Ongoing research focuses on residual stress measurement using micro-piezospectroscopy and more rigorous theoretical studies to understand the microchemistry of these systems.

4. DISCUSSION

4.1. Influence of residual stresses on the interfacial debonding behavior

Residual stresses in these whisker/glass systems arise from the thermal–mechanical mismatch between the two constituents and can be calculated based on the properties of the β-Si_3N_4 [19, 20] and the oxynitride glasses [21] using a modified Eshelby

model [22, 23]. Details of the stress analyses model can be found in Refs [22, 23]. These stress analyses revealed that the radial and axial stresses imposed on a rod embedded in oxynitride glass were compressive, primarily due to the lower thermal expansion coefficient of silicon nitride. Recent preliminary micro-piezospectroscopy results from two samples (AlY20-I and YAl20-I) indicate that the measured and the calculated stress levels in the β-Si_3N_4 whiskers are of the same order of magnitude [24]. An earlier study on Y-bearing Si–Al–Y–O–N systems found that there was little, if any, dependence of the θ_{crit} values on the radial residual stresses imposed on the whisker/glass interfaces [12]. It was concluded that the residual stresses were not a significant factor in the observed debonding behavior in those Si–Al–Y–O–N systems [12]. In the present study, the role of residual stress on the interfacial debonding behavior is assessed further.

The thermal and mechanical properties of the glasses and the β-Si_3N_4 crystal used in the present study are listed in Table 2. Poisson ratios of the whiskers and glasses were assumed to be 0.29 and 0.26, respectively, and the aspect ratio of the whisker was assumed to be 10. Stresses normal to the long axis of the whisker were calculated and are listed in Table 2. These calculated stresses can be approximated as the radial stresses imposed on the whisker/glass interface because of the relatively high aspect ratio of the whiskers. The circumferential stresses were not analyzed because they could not have a significant influence on the interfacial debonding behavior. The relationship between the residual stresses and the θ_{crit} and l_{db} values are shown in Fig. 4(a) and (b). The θ_{crit} values appear to decrease slightly with increasing radial compressive stress imposed on the interface [Fig. 4(a)]. However, the formation of an epitaxial SiAlON interfacial layer dominates the θ_{crit} values as compared to the influence of the residual stresses. In the absence of an epitaxial SiAlON layer, increases in the compressive radial residual stress level imposed on the interfaces substantially reduce the debond length for a given θ value [Fig. 4(b)]. Note that between these two parameters, θ_{crit} is the prime factor while l_{db} serves a second order but important factor, as explained in Section 2. Therefore, in the whisker/oxynitride-glass systems examined here, interfacial chemistry/microstructure is a more dominant influence than the residual stress imposed on the interface by the thermal–mechanical mismatch between the whisker and the glass. The residual stresses, however, do have an impact on the interfacial debonding behavior by, at least, affecting the debonding length, when no epitaxial SiAlON layer formed on the β-Si_3N_4 whisker.

4.2. Influence of the SiAlON composition on the interfacial debonding behavior

It is not just the presence of the epitaxial SiAlON layer but also the composition of the SiAlON, specifically the Al and O concentration in the SiAlON layer, that influence the debonding behavior of the whisker/oxynitride-glass interface. This finding was obtained by relating the interfacial debonding behavior in these whisker/glass systems to the fracture behavior of seeded silicon nitrides. Self-reinforced silicon nitrides with fixed microstructures were processed using a seeding method followed by tape casting [25]. The fracture behavior of seeded silicon nitrides densified using different yttria and alumina additive ratios has been reported in

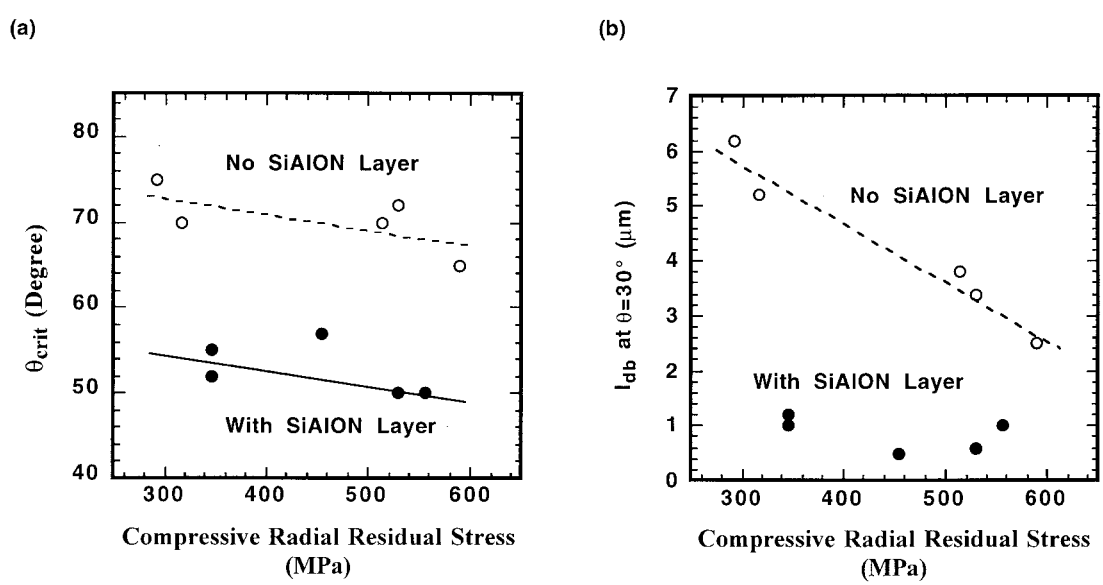

Fig. 4. The relationship between the compressive radial residual stresses imposed on the whisker/glass interface and (a) the θ_{crit} and (b) the l_{db} values.

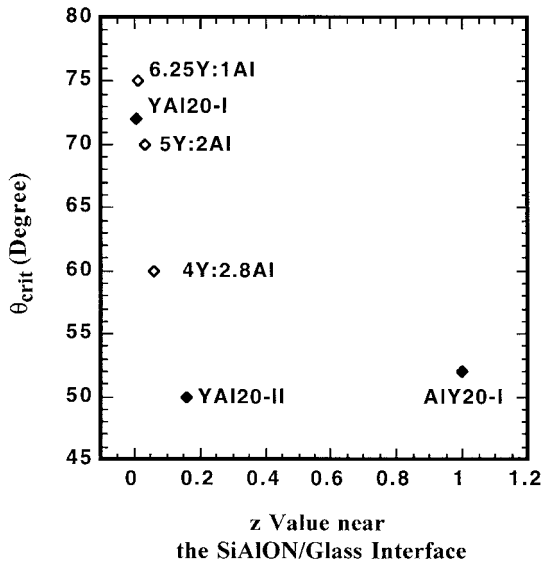

Fig. 5. Variation of θ_{crit} as a function of the z-value of the β'-$Si_{6-z}Al_zO_zN_{8-z}$. (Open symbols are data from the seeded silicon nitrides [26] and filled symbols are data from the whisker/glass systems. The seeded silicon nitrides are labeled by the Y:Al ratio (in wt%) employed in the sintering additives [26].) Note the θ_{crit} value decreases most rapidly in the low z region (≤ 0.2) and appears to be approaching an asymptote at high z-values.

detail earlier [26]. The Al and O concentrations in the β'-$Si_{6-z}Al_zO_zN_{8-z}$ growth layer in the seeded silicon nitrides ($z \leq 0.11$) were lower than those in the whisker/glass systems, mainly due to the small amount of glass and hence the limited supply of Al and O. In the seeded silicon nitrides, measurements of θ_{crit} were obtained during *in situ* observation of the interaction of cracks with the elongated grains, utilizing an applied moment double cantilever beam (DCB) testing stage. Plotting θ_{crit} vs the z-value of the corresponding β'-$Si_{6-z}Al_zO_zN_{8-z}$ phase, it was found that data from the whisker/glass model systems (AlY20-I, YAl20-I, and YAl20-II) and from the seeded silicon nitrides follow the same trend, as shown in Fig. 5. Note the θ_{crit} value decreased most rapidly in the low z region (≤ 0.2) and appeared to be approaching an asymptote at high z-values. This explains why the fracture toughness of the seeded silicon nitride is sensitive to the z-value [26] while no significant difference in the interfacial debonding behavior is observed in the whisker/glass model systems with β'-SiAlON growth layers of relatively high z-values ($z > 0.2$).

In general, important features in compositional dependence of the debonding behavior can be rationalized on the basis of the atomic bonding across the whisker/glass interface. This is most clear for the $z = 0$ limit, when the crystal in contact with the glass is silicon nitride. For the whisker/glass interface without SiAlON formation, β-Si_3N_4 supports only $Si_{Si_3N_4}$–O_{glass} cross-bonds (heteronuclear bonds "crossing" the crystal/glass interface), in addition to the majority Si–N cross-bonds. However, incorporation of Al and O in the lattice to form β'-SiAlON not only increases the number and type of Si–O cross-bonds with a new possibility for Si_{glass}–O_{SiAlON} linkages, but also introduces Al–O cross-bonds of both types (Al_{SiAlON}–O_{glass} and Al_{glass}–O_{SiAlON}). This is a strengthening step on the simple conceptual basis of bond strengths in Si and Al oxides, and it is further supported by local density [27] studies of basic tetrahedral clusters. From first-principles studies of small atomic tetrahedral clusters [28], it is found that the Si–O bond is the most energy lowering (hence strongest) bond and the Al–O bond is stronger than the Al–N bond. As shown in Fig. 6, the binding energy (relative to dissociated atoms) of SiN_xO_y and AlN_xO_y tetrahedral

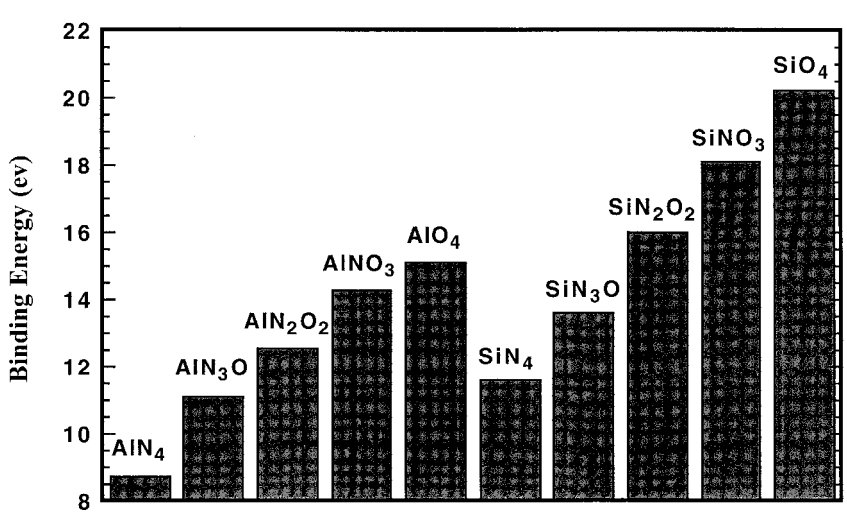

Fig. 6. Histogram of calculated binding energies of five-atom Si and Al tetrahedral clusters with various O/N compositions.

clusters increases systematically when O substitutes for N in both series, with SiO_4 being the most energetically stable unit. The tetrahedra were isotropically relaxed in each case. Among all the tetrahedral structures, SiO_4, $SiNO_3$, SiN_2O_2 and AlO_4 are more stable than the others, as shown in Fig. 6. This result agrees with an NMR study on Si–Al–Y oxynitride glasses which shows that the glasses are built up of $Si(O_4)$, $Si(O_3N)$, $Si(O_2N_2)$ and $Al(O_4)$ tetrahedras [29]. Therefore, the key point concerning Al and O additions to β-Si_3N_4 in the β'-SiAlON interlayer is the formation of energy lowering, stronger bonds across the SiAlON/glass interface. As mentioned earlier, this is most apparent near the $z = 0$ limit, where each O atom added into the SiAlON surface introduces an additional Si–O or Al–O cross-bond. As replacements for cross-bonds of Si–N and Al–N type, these would enhance the interfacial cohesion.

Note that substitution of Al for Si at a particular interface site without changing the coordination to neighboring atoms would actually weaken the bond across the interface, because a Si atom is more strongly bound than an Al atom for a given coordination sphere O_xN_y. However, the strong association for Al to bond with O to the exclusion of N suggests Al will occur at the interface preferentially at "O-rich" sites, where Al–O bonds are strong. As illustrated in Fig. 6, whereas AlN_4 and AlN_3O are less stable than all Si-bonded clusters, $AlNO_3$ and AlO_4 are in fact stronger than SiN_4 and SiN_3O. Therefore, the displacement of Si atoms at the SiAlON surface would not necessarily cause an overall weakening of interfacial strength. Also note that the possibility of forming Al–N cross-bonds is relatively small, because of the strong association of O with Al. As shown in Fig. 6, AlN_4 is least energetically favorable. Previous studies lend support to this, as it is found that Si–O, Si–N and Al–O are the major bonds in Si–Al–Y oxynitride glasses [29–31], although the presence of Al–N bonds cannot be completely ruled out [31].

To conclude, the bonding strength at the β'-SiAlON/Si–Y–Al-oxynitride-glass interface is influenced by the Al and the O concentrations in the β'-SiAlON layer. Increasing Al and O contents in the β'-SiAlON growth layer makes the compositional transition across the SiAlON/glass interface more continuous. Atomic cluster results suggest this enhances the number of strong chemical bonds (i.e. Si–O and Al–O) across the interface, thus making debonding more difficult. This preliminary result from first-principles studies of the basic tetrahedral fragments of the system is consistent with the experimental observations. Currently, further theoretical and experimental work is being carried out to understand the basic structure and properties of amorphous intergranular films and their interfaces with crystalline grains.

5. CONCLUSIONS

The debonding behavior at interfaces between β-Si_3N_4 whiskers and oxynitride glasses was investigated. Two groups of glasses were employed: Y-bearing Si–Al–Y–O–N glasses and Ln-bearing Si–Al–Ln–O–N glasses. It was found that in both the Y-bearing Si–Al–Y–O–N systems and the Ln-bearing Si–Al–Ln–O–N systems, formation of an epitaxial $Si_{6-z}Al_zO_zN_{8-z}$ growth layer on the β-Si_3N_4 whiskers significantly increased the interfacial debonding strength. The interfacial debonding strength was very sensitive to the Al and O concentrations in the SiAlON layers. The debonding strength increased rapidly with increasing z in the low-z region. In the Ln-bearing systems, in addition to SiAlON formation, the Ln ions modify the debonding behavior by varying the debonding length. Compared to interfacial chemistry, residual stresses imposed on the interface due to thermal–mechanical mismatch were only a secondary influence on the debonding behavior, modifying the debonding length in systems without SiAlON formation. First-principle studies indicated that incorporation of O and Al into the β-Si_3N_4 lattice structure (SiAlON formation) induces strong Si–O and Al–O bonds across the whisker/glass interface, thus enhancing the interface strength. The results from the present study suggest that the interfacial debonding behavior is strongly influenced by the nature of the chemical bonding at the interface. The fracture resistance of silicon nitride can be improved by controlling the densification additives employed and hence tailoring the chemistry of the intergranular glassy phase.

Acknowledgements—This research was sponsored by the U.S. Department of Energy, Division of Materials Sciences, Office of Basic Energy Sciences, under contract DE-AC05-96OR22464 with Lockheed Martin Energy Research Corp. The authors thank Drs I. M. Anderson and M. J. Lance for reviewing the manuscript. This work is also in cooperation with the International Group for the Fundamentals of Inter-Granular Films (IGF)[2].

REFERENCES

1. Lange, F. F., *J. Am. Ceram. Soc.*, 1979, **62**, 428.
2. Tani, E., Umebayashi, S., Kishi, K. and Nishijima, M., *Am. Ceram. Soc. Bull.*, 1996, **65**, 1311.
3. Li, C. W. and Yamanis, J., *Ceram. Engng Sci. Proc.*, 1989, **10**, 632.
4. Hoffmann, M. J. and Petzow, G., *Mater. Res. Soc. Symp. Proc.*, 1993, **287**, 3.
5. Becher, P. F., Sun, E. Y., Plucknett, K. P., Alexander, K. B., Hsueh, C. H., Lin, H. T., Waters, S. B. and Westmoreland, C. G., *J. Am. Ceram. Soc.*, 1998, **81**, 2821.
6. Becher, P. F., Hwang, S. L. and Hsueh, C. H., *MRS Bull.*, 1995, **XX**, 23.
7. Peterson, I. M. and Tien, T. Y., *J. Am. Ceram. Soc.*, 1995, **78**, 2345.
8. Tajima, Y., Urashima, K., Watanabe, M. and Matsuo, Y., *Ceramic Transactions, Vol. 1: Ceramic Powder Science—IIB*, ed. G. L. Messing, E. R. Fuller,

Jr and H. Hausner. American Ceramic Society, Westerville, OH, 1988, p. 1034.
9. Tajima, Y., *Mater. Res. Soc. Symp. Proc.*, 1993, **287**, 189.
10. Urashima, K., Tajima, Y. and Watanabe, M., *Fracture Mechanics of Ceramics*, Vol. 9, ed. R. C. Bradt. Plenum Press, New York, 1992, p. 235.
11. Wötting, G. and Ziegler, G., *Ceramics Int.*, 1984, **10**, 18.
12. Becher, P. F., Sun, E. Y., Hsueh, C. H., Alexander, K. B., Hwang, S. L., Waters, S. B. and Westmoreland, C. G., *Acta mater.*, 1996, **44**, 3881.
13. Kramer, M., Hoffmann, M. J. and Petzow, G., *J. Am. Ceram. Soc.*, 1993, **76**, 2778.
14. He, M. Y. and Hutchison, J. W., *Int. J. Solids Struct.*, 1989, **25**, 1053.
15. Becher, P. F., Hsueh, C. H., Alexander, K. B. and Sun, E. Y., *J. Am. Ceram. Soc.*, 1996, **79**, 298.
16. Sun, E. Y., Alexander, K. B., Becher, P. F. and Hwang, S. L., *J. Am. Ceram. Soc.*, 1996, **79**, 2626.
17. Drew, A., *Nitrogen Glass, Research Reports in Materials Science*, ed. P. E. Evans. The Puthenon Press, Casterton Hall, U.K., 1986.
18. Nakayasu, T., Yamada, T., Tanaka, I., Adachi, H. and Goto, S., *J. Am. Ceram. Soc.*, 1998, **81**, 565.
19. Henderson, C. M. B. and Taylor, D., *Trans. Br. Ceram. Soc.*, 1975, **74**, 49.
20. McCreight, L. R., Rauch Sr, H. W. and Sutton, W. H., *Ceramic and Graphite Fibers and Whiskers*. Academic Press, New York, 1965.
21. Sun, E. Y., Becher, P. F., Hwang, S. L., Waters, S. B., Pharr, G. M. and Tsui, T. Y., *J. Non-Cryst. Solids*, 1996, **208**, 162.
22. Hsueh, C. H. and Becher, P. F., *Mater. Sci. Engng*, 1996, **A212**, 22.
23. Li, Z. and Bradt, R. C., *J. Am. Ceram. Soc.*, 1989, **72**, 70.
24. Dauskardt, R., Unpublished results.
25. Hirao, K., Nagaoka, T., Brito, M. E. and Kanzaki, S., *J. Am. Ceram. Soc.*, 1994, **77**, 1857.
26. Sun, E. Y., Becher, P. F., Plucknett, K. P., Hsueh, C. H., Alexander, K. B. and Waters, S. B., *J. Am. Ceram. Soc.*, 1998, **81**, 2831.
27. Jones, R. O. and Gunnarsson, O., *Rev. mod. Phys.*, 1989, **61**, 689.
28. Painter, G. S., Unpublished results.
29. Aujla, R. S., Leng-Ward, G., Lewis, M. H., Seymour, E. F. W., Styles, G. A. and West, G. W., *Phil. Mag. B*, 1986, **54**, L51.
30. Loehman, R. E., *J. Am. Ceram. Soc.*, 1979, **62**, 491.
31. Sato, R. K., Bolvin, J. and McMillan, P. F., *J. Am. Ceram. Soc.*, 1990, **72**, 2494.